Modelling the transverse behaviour of circular tunnels in structured clayey soils during earthquakes

Title:

Modelling the transverse behaviour of circular tunnels in structured clayey soils during earthquakes

Authors:

Lowell Tan Cabangon[1], Gaetano Elia[2], Mohamed Rouainia[3]

[1] Ph.D. candidate, School of Engineering, Newcastle University, NE1 7RU Newcastle Upon Tyne, UK. E-mail: l.t.cabangon1@newcastle.ac.uk

[2] Tenure-track Associate Professor in Geotechnical Engineering (Ph.D.), Department of Civil, Environmental, Land, Building Engineering and Chemistry (DICATECh), Technical University of Bari, via Orabona 4, 70125 Bari, Italy – formerly School of Civil Engineering & Geosciences, Newcastle University, NE1 7RU Newcastle Upon Tyne, UK. (Corresponding Author) E-mail: gaetano.elia@ncl.ac.uk, gaetano.elia@poliba.it; Phone: +39 0805963693

[3] Reader in Computational Geomechanics (Ph.D.), School of Engineering, Newcastle University, NE1 7RU Newcastle Upon Tyne, UK. E-mail: mohamed.rouainia@ncl.ac.uk

Abstract

The paper presents novel results from advanced numerical simulations of the transverse behaviour of shallow circular tunnels in natural clays accounting for soil structure degradation induced by earthquake loading. It combines the calibration of a kinematic hardening model against real laboratory data with outputs from a parametric study with different degradation rates of soil structure to demonstrate the good performance of the model and draw conclusions of significance to both researchers and designers. The sensitivity analysis indicates an increase in the maximum and minimum values of the lining forces attained during the earthquake motions and in the lining hoop force and bending moment increments in response to the seismic events when higher rates of destructuration are accounted for. Hence, the paper highlights for the first time the importance of the initial structure and its degradation in controlling the magnitude of the tunnel lining forces and, consequently, the overall seismic tunnel design.

Keywords:

Tunnels; Earthquakes; Finite element method; Constitutive models; Natural clays; Destructuration.

1. Introduction

The urban population is predicted to rise to more than 6 billion by 2045, with the largest growth occurring in countries of known seismicity, such as China, India and Indonesia [1]. The need for space within cities with growing population has recently seen an increase in urban regeneration projects as well as construction of new underground services and transport links. In this context, urban tunnels are considered “lifeline” utilities as their continued operation is of vital importance during and in the immediate aftermath of an earthquake. It is, therefore, imperative to assess the engineering performance of such important geotechnical structures to ensure their resilience during and after seismic events.

Failures of geotechnical structures due to earthquake events, with huge consequences in terms of fatalities and financial costs, have been widely documented in recent years. These failures are often associated with significant deformation of soil deposits which can cause major damage to buildings and surface infrastructure facilities. On the contrary, dynamic effects on underground structures have often been neglected based on the assumption that their response to earthquake loading is relatively safe. Nevertheless, several examples of recorded damage to underground structures for which seismic forces were not considered in the original design can be found in the literature. Hashash *et al*. [2] described the collapse of the Daikai subway station in Kobe during the 1995 Hyogoken-Nambu earthquake, the damages to highway tunnels in Central Taiwan during the 1999 Chi-Chi earthquake and the collapse of the Bolu tunnel in Turkey during the 1999 Düzce earthquake. Twelve per cent of the mountain tunnels in the epicentral area were heavily damaged during the Kobe earthquake [3], while after the Chi-Chi earthquake 26% of the 50 tunnels located within 25 km of the rupture zone were severely damaged and 22% moderately damaged [4]. More recently, Li [5] reported the investigation of seismic damages to 11 highway tunnels in the Yingxiu Town area during the Wenchuan earthquake occurred on May 2008: 4 were seriously damaged, 3 moderately damaged and 4 slightly damaged. The main causes of damage in these case histories

were the shallow depth of tunnels, the poor geological conditions (i.e. soft soils with high plasticity, weak rocks), the displacement of active faults crossing the tunnel and pre-existing structural defects in the tunnel lining. During a seismic event, tunnels are subjected to axial compression and extension, longitudinal bending and ovaling or racking of the tunnel lining [6]. Underground facilities constructed in soft soils or weak rocks, such as urban tunnels, can be expected to suffer more damage compared to openings constructed in competent rocks [2]. Ovaling and racking of the tunnel lining are reported to be the most critical sources of damage [7], although longitudinal effects may have a significant impact on the response of long underground structures [2, 8].

The seismic design of tunnels has been addressed in the past by a number of researchers who have proposed solutions based on analytical or numerical investigations. The analytical design methods typically rely on elasticity solutions to calculate the dynamic lining forces a tunnel experiences during an earthquake event and generally ignore the inertial effects [e.g. 9-10]. The Soil-Structure Interaction (SSI) approach has, instead, the ability to consider relatively complex conditions in terms of heterogeneity of soil strata, non-regularity of tunnel geometry, pre-existence of surface and sub-surface structures, ground water flow. In such cases, the analysis of SSI can take advantage of the use of numerical two-dimensional (2D) and three-dimensional (3D) approaches, like the boundary element (BE) method and the finite element (FE) method. Most commonly, the problem is modelled in the transverse direction only, assuming plane strain conditions [e.g. 11-17]. However, when the direction of wave propagation is arbitrary with respect to the axis of the structure the problem becomes three-dimensional and few contributions studying this aspect can be found in literature [e.g. 18-22]. The capabilities of such numerical approaches in assessing tunnels behaviour under seismic loading have not been fully exploited, as they require the use and calibration of advanced constitutive models to appropriately describe the soil stress-strain behaviour during the dynamic action. In particular, the evolution of microstructure (destructuration) induced in natural soil deposits by the seismic action, and its effect on the soil-tunnel dynamic behaviour has

never been investigated before.

In this paper the dynamic performance of a shallow circular tunnel in a natural clay deposit is analysed by means of a 2D non-linear FE approach. The calibration of an advanced kinematic hardening multi-surface soil model against real laboratory data is firstly presented. Different rates of destructuration of the soil initial structure are assumed in the calibration phase to investigate, for the first time, the effects induced by structure degradation on the soil-tunnel behaviour in dynamic conditions. The geometrical and geotechnical properties of the numerical model are then discussed along with the selection strategies for the definition of the bedrock input motions. The soil-tunnel interaction during the seismic events is, in turn, described by presenting the profile of maximum accelerations within the deposit, the stress-strain soil response, the structure degradation process induced by the seismic motions and the evolution with time of the excess pore pressures throughout the earthquake events. Finally, the distribution and time histories of the lining forces induced in the tunnel by the input motions are presented for the different cases and some conclusions are drawn at the end.

2. Soil constitutive model

To accurately predict the behaviour of tunnels during earthquakes through FE analyses, it is crucial to use a constitutive model that can appropriately capture the soil response to seismic loads. In common engineering practice and design, simple constitutive assumptions (e.g. Mohr-Coulomb) are often employed to model the stress-strain behaviour of the soil deposit. However, these constitutive hypotheses are not adequate to simulate the main features of the mechanical behaviour of soils during cyclic loading such as non-linearity, early irreversibility, decrease of nominal stiffness, hysteretic energy dissipation and pore pressure build-up in undrained conditions. Ignoring these effects can lead to an incorrect prediction of the ground deformations, especially in soft soil deposits subjected to dynamic loading, thus resulting in an inappropriate design of the tunnel lining.

In this work the kinematic hardening model (*RMW*) developed by Rouainia and Muir Wood [23] has been employed to simulate the cyclic response of natural clay materials. It contains three surfaces: 1) a reference surface, which controls the state of the soil in its reconstituted, structureless form and describes the intrinsic behaviour of the clay; 2) a structure surface, which controls the process of destructuration; 3) a bubble, which encloses the elastic domain of the soil and moves within the structure surface following a kinematic hardening rule. The degree of structure, *r*, which describes the relative sizes of the structure and reference surfaces, is a monotonically decreasing function of the plastic strain, thus representing the progressive degradation of the material. The model converges to the Modified Cam-Clay model for remoulded structureless soils once the three surfaces are set to be coincident. The *RMW* model has been successfully employed to simulate both static [24-25] and dynamic geotechnical problems [26-27]. It has been implemented in PLAXIS 2D [28] with an explicit stress integration algorithm adopting an automatic sub-stepping and error control scheme [29]. The model has been calibrated against a series of laboratory results reported by Burghignoli *et al*. [30], D'Elia [31] and Burghignoli *et al*. [32] for Avezzano Clay, a structured Italian clay. The Avezzano deposit is in a highly seismic area of central Italy and could potentially be the location of underground infrastructure and transport links in the future. Specifically, the site considered is in the Fucino basin, a large intra-mountain depression located 80km east of Rome and surrounded by the Apennines. The basin has originated from the sedimentation of fluvio-lacustrine sediments during the Pleistocene period and is composed by top layers of clayey and silty soils, with sand and gravel found underneath. The deposit is geologically normally consolidated and the silty clay layers are characterised by very low plasticity (PI of about 10%) and high values of calcium carbonate content (i.e. $CaCO_3$ content between 60 and 80%). Standard oedometer and undrained triaxial compression tests clearly indicate that the clayey layers are characterised by the typical mechanical behaviour of cemented clays [30, 32]. The response of the deposit in Avezzano to cyclic loads imposed by a silo shallow foundation has been investigated in the past by

Burghignoli *et al*. [30], D'Elia *et al*. [33], Burghignoli *et al*. [34] and, more recently, Elia and Rouainia [27] evaluated the performance of the same footing under seismic loading conditions. In this work, the undrained triaxial compression tests on Avezzano Clay natural samples retrieved at depths of 15 and 21m have been considered. Figure 1 shows the comparison in terms of stress paths, stress-strain and pore pressure-strain response between the laboratory data from [32] and the numerical predictions obtained with *RMW*. For the same set of experimental data shown in the figure, the constitutive model has been calibrated following the work by [27, 34], considering an initial degree of structure r_0 equal to 5.2 and two rates of destructuration with damage strain (i.e. two values of the parameter k). The numerical prediction obtained assuming k equal to 1.5, presented in Figure 1, is in very good agreement with the laboratory data, whereas the strain-softening will be more abrupt than in the experiments when a higher rate of destructuration (k = 5.0) is adopted. In previous versions of *RMW* a classical hypoelastic formulation was employed for the determination of the bulk and shear moduli, K and G_0. In this work, the well-known equation proposed by Viggiani and Atkinson [35] for the small-strain shear modulus has been implemented to reproduce the dependency of G_0 on the mean effective stress and overconsolidation ratio. It should be noted that the adopted elastic formulation cannot predict the influence of structure on the initial elastic stiffness, as recently proposed by Elia and Rouainia [36]. Consistently with the Avezzano Clay plasticity index of 10%, the dimensionless stiffness parameters A, n and m in the equation proposed by Viggiani and Atkinson [35] have been set equal to 2150, 0.78 and 0.22, respectively. The small-strain stiffness response and the evolution of the shear modulus and damping ratio of Avezzano Clay has been experimentally investigated and reported by D'Elia [31]. In particular, Figure 2 shows the normalised modulus decay and damping curves obtained from double specimen direct simple shear (DSDSS) and combined resonant column/torsional shear (RC/TS) tests performed on natural Avezzano Clay samples, which were retrieved from the top part of the deposit (i.e. at depths between 8 and 11m). Numerical simulations of strain-controlled

undrained cyclic simple shear tests have been carried out in order to calibrate the *RMW* parameters, which control the reduction of shear modulus and the evolution of the damping ratio with cyclic shear strain [e.g. 36]. The model predictions, presented in the same Figure 2, are in good agreement with the laboratory data when the lower rate of destructuration is accounted for. Associated with a more pronounced strain-softening response, the normalised stiffness modulus for k equal to 5.0 decays quicker than that obtained assuming a destructuration rate equal to 1.5 over the entire strain range and underestimates the experimental data. In contrast, a very small difference can be observed in terms of hysteretic damping predicted by the model in the two cases.

A summary of the *RMW* model parameters resulting from the calibration and adopted in the FE non-linear dynamic simulations undertaken in this work is reported in Table 1.

3. Numerical model

The case of a shallow circular tunnel, 10m in diameter with 15m soil cover, within a normally consolidated 70m thick deposit of Avezzano Clay overlying a rigid bedrock has been considered, using the soil model parameters derived from the above calibration procedure. The lining has been assumed to be made by precast concrete segments 0.5m thick and it has been modelled as a linear visco-elastic material with Young's modulus equal to 38GPa, Poisson's ratio equal to 0.25 and damping ratio equal to 5%. Standard boundary conditions have been adopted for the static analyses, while the bottom of the model has been assumed rigid and equal displacements have been imposed to the nodes along the vertical sides of the mesh (i.e. tied-nodes lateral boundary conditions). Tied-nodes have been employed for the dynamic simulations in order to avoid spurious wave reflections at the boundaries of the soil deposit. Their effectiveness in absorbing the energy induced by the seismic action has been proved by Zienkiewicz *et al.* [37]. In addition, a parametric study of the FE model length has shown that the adopted horizontal dimension (i.e. 350m), equal to 5 times the deposit depth as suggested by Amorosi *et al*. [38], in conjunction with the tied-node boundaries, is

sufficient to properly simulate the free-field conditions at the edges of the model. The water level has been assumed to coincide with the ground surface. Figure 3 shows the geometry of the FE model adopted in PLAXIS 2D [28] along with the dynamic boundary conditions. As in previous works [27, 34], a coefficient of earth pressure at rest K_0 equal to 0.5 has been assumed in the generation of the geostatic stress state, using a unit weight of 18kN/m^3 for the clay. The G_0 profile resulting from the equation proposed by Viggiani and Atkinson [35] is shown in the same figure and compared with RC data on Avezzano Clay presented by Burghignoli *et al*. [34]. The FE model has been discretised with a total number of 5088 15-noded plane strain triangular elements, with the mesh refined in the region around the tunnel to avoid mesh sensitivity due to the softening behaviour predicted by the *RMW* model. To ensure that the seismic wave transmission is represented accurately through the finite element mesh, the vertical distance between adjacent element nodes has been limited to satisfy the condition recommended by Kuhlemeyer and Lysmer [39], even when the reduction of the initial shear modulus during the dynamic excitation produces a reduction in the wave length. A static analysis under undrained conditions has been initially performed to simulate the tunnel excavation and installation of the tunnel lining. A contraction equivalent to 0.8% volume loss, deemed to be acceptable for a satisfactory performance of the tunnel excavation [e.g. 40], has been imposed. The dynamic analyses have been carried out under undrained conditions with a time step corresponding to that of the earthquake input signals. In the dynamic simulations only 2% Rayleigh damping has been added to avoid the propagation of spurious high frequencies and to compensate for the *RMW* underestimation of damping in the small-strain range, using the calibration procedure proposed by Amorosi *et al*. [38].

Two earthquake signals, both reasonably matching the response spectrum provided by Eurocode 8 (EC8) for soil type A, have been considered in the dynamic simulations, as illustrated in Figure 4. The first signal was recorded at the Assisi-Stallone station during the Umbria-Marche earthquake in September 1997, while the second was recorded at the Ulcinj-Hotel Albatros station during the

Montenegro earthquake in April 1979. The Montenegro earthquake has been selected to explicitly match EC8 for the first natural period of the soil deposit, T_1 (equal to 1.03s) calculated according to the viscoelasticity theory [e.g. 41]. This value represents only an initial guess of the first oscillation mode of the soil deposit and it is used to guide the selection process of the input motion and the interpretation of the non-linear dynamic analyses presented in the following. Actually, from Figure 4 it is evident that the Montenegro signal is characterised by much higher spectral accelerations at around T_1 with respect to the Umbria-Marche earthquake, thus implying a higher energy content applied to the system at its first oscillation mode. The relevant characteristics of the selected acceleration time histories are listed in Table 2 in terms of magnitude (M_W), Arias Intensity (I_a) as proposed by Arias [42], epicentral distance, effective duration (T_{90}) as defined by Trifunac and Brady [43], maximum acceleration ($a_{\max}$) and maximum velocity ($v_{\max}$). Both input motions have been filtered to prevent frequencies higher than 10Hz and scaled up to the same peak acceleration (PGA) of 0.30g, according to the seismic hazard analysis of the site presented by Elia and Rouainia [27]. They have been applied at the base of the mesh as prescribed horizontal displacement time histories.

4. Results and discussion

In this section, the soil-tunnel interaction response during the selected earthquake events has been systematically investigated to highlight the influence of the initial degree of structure and its subsequent degradation induced by the seismic loads. Specifically, two sets of simulations have been considered and compared: the ones performed applying the two input motions and using a rate of destructuration equal to 1.5 and those in which the *RMW* parameter *k* has been set equal to 5.0. In the following, the results of the dynamic analyses are presented in terms of propagation of the seismic waves within the deposit, mechanical response of the soil surrounding the tunnel and distribution and time histories of the lining forces induced in the tunnel by the earthquake actions.

The profiles of maximum horizontal acceleration recorded along the tunnel vertical and in free field conditions (with location shown in Figure 3) during the two selected earthquake events are presented in Figure 5. For both seismic events and along both verticals, the FE analyses predict an overall deamplification of the bedrock motion at surface. It also seems that the degradation rate does not particularly influence the wave propagation in the deposit. Moreover, it appears that the Montenegro input motion induces higher accelerations, especially in the bottom part of the deposit and below the tunnel, but the PGA at surface is similar to the one recorded during the Umbria-Marche event. These findings are confirmed by the response spectra of the accelerations recorded at ground surface along the tunnel vertical and in free field conditions shown in Figure 6 and compared with the response spectra of the input motions applied at bedrock. In general, given the higher energy content of the Montenegro event at T_1 (see Figure 4) significantly higher shear strain levels are induced in the deposit than those by the Umbria-Marche seismic motion.

The stress-strain curves recorded in free field conditions during the two seismic events at different depths (i.e. at 10, 15, 25 and 50 m from the ground surface) and assuming two rates of destructuration are presented in Figure 7. The shear strains induced by the Montenegro earthquake, ranging between about 0.5% at the surface and 0.25% at depth, are at least double the corresponding strains associated to the Umbria-Marche event. The figure also shows a softer behaviour of the soil when the rate of destructuration assumed in the simulations is higher (i.e. for k = 5.0), consistently with the normalised stiffness modulus curves presented in Figure 2.

For the case of k = 1.5, the evolution with time of the shear strains recorded during the two seismic events around the tunnel is shown in Figures 8a and 8d as function of the angle θ (defined positive in the anti-clockwise direction). The non-symmetric response observed in terms of shear strains is the counterpart of an elasto-plastic behaviour induced in the soil deposit by the dynamic excitation. In addition, Figures 8b and 8e show the time histories of excess pore water pressures predicted along the tunnel vertical for the Umbria-Marche and Montenegro events, respectively. The FE non-

linear analyses predict the build-up of positive pore pressures above the tunnel and negative pressures below it, associated with the accumulation of permanent soil deformations and structure degradation throughout the two earthquake motions. Higher excess pore pressures are recorded during the Montenegro event, ranging between 100kPa at 25m depth and -27kPa at the bottom of the mesh. The evolution with time of the *RMW* parameter *r*, describing the degree of soil structure, during the two seismic motions is shown in Figures 8c and 8f for three different locations around the tunnel. More pronounced structure degradation is induced in the soil surrounding the tunnel by the Montenegro seismic event, consistently with the higher shear strain levels and excess pore pressures recorded during this earthquake in the same locations. Figure 9 shows the contours of *r* obtained at the end of the two seismic events, indicating a more diffused destructuration occurred in the soil deposit during the Montenegro analysis compared to the Umbria-Marche case. Moreover, in both cases higher destructuration is observed in the top part of the model, between the tunnel and ground surface, where the deamplification of the input signal occurs (see Figure 5).

Figure 10 presents the time histories of shear strain, excess pore pressure and *RMW* structure parameter *r* during the two earthquake events when a destructuration rate of 5.0 is adopted in the simulations. The higher degree of destructuration allowed in the simulations leads to the development of higher shear strains around the tunnel (Figures 10a and 10d) and the consistent accumulation of positive pore water pressures in the soil deposit (Figures 10b and 10e), reaching a maximum value of excess pressure almost equal to 200kPa in the Montenegro analysis. Almost a full structure degradation is observed at $\theta = 90°$ when the Montenegro input motion is applied at bedrock (i.e. *r* approaches a final value of 1.0), as indicated by Figure 10f. This is confirmed by the contours of *r* obtained at the end of the two seismic events, shown in Figure 11, where full destructuration of the top 5m of the soil deposit can be observed in the Montenegro case.

Moving to the tunnel dynamic behaviour, Figure 12 shows the distribution of hoop force *N*, bending moment *M* and shear force *Q* before and after the seismic events as function of the angle θ for a

destructuration rate k = 1.5. The standard convention of structural analysis (i.e. compression is negative) is adopted here when presenting the results in terms of lining forces. The envelopes of maximum and minimum values of N, M and Q during the earthquake events are also shown in the same figure with dashed lines. For both input motions, the use of elasto-plastic models allows to predict permanent increments of hoop force (ΔN), bending moment (ΔM) and shear force (ΔQ) at the end of the motions due to the accumulation of plastic deformation in the soil deposit during the earthquakes, as already observed by other researchers [14, 16, 17]. The lining forces predicted at the end of the Montenegro analyses (Figures 12d - 12f) are larger than those recorded at the end of the Umbria-Marche simulations (Figures 12a - 12c). This can be attributed to the higher accelerations induced by the Montenegro signal at tunnel location (see Figures 5a and 5b). The corresponding distribution of lining forces obtained for a destructuration rate equal to 5.0 are reported in Figure 13. With respect to the case of k = 1.5, higher hoop forces, bending moments and shear forces are induced in the tunnel, especially by the Montenegro earthquake, when a higher degree of destructuration is allowed to occur in the dynamic analyses. Finally, Figure 14 shows, for the two destructuration rates assumed, the time histories of hoop force and bending moment increments during the Umbria-Marche event at θ equal to 0°, 45°, 90° and 135°, whereas the evolution with time of ΔN and ΔM predicted at the same lining locations throughout the Montenegro event is reported in Figure 15. The sensitivity analysis indicates that the assumption of a higher destructuration rate can significantly affect the lining forces, causing a consistent increase of hoop force and bending moment increments accumulated in the tunnel lining during both earthquake scenarios. This rise is due to the softer response of the soil characterised by a higher rate of destructuration (Figure 2), which, in turn, causes the transmission of higher loads to the tunnel lining.

Overall, the simulation results highlight the importance of the input motion frequency content in controlling the magnitude of shear strains induced by the earthquake in the tunnel and surrounding

deposit. The parametric analysis points out a consistent increase in the hoop force and bending moments increments accumulated in the tunnel lining when a higher degree of destructuration is allowed to occur in the dynamic simulations.

5. Conclusion

The paper describes a set of non-linear FE analyses for the simulation of the transverse behaviour of a shallow circular tunnel in a typical natural clay deposit subjected to earthquake loading. Starting from the same set of laboratory test results on a real natural clay, different assumptions on the degradation rate of the initial soil structure are made in the calibration of an advanced constitutive model used to describe the clay dynamic behaviour. Two input motions, scaled to the same peak acceleration but characterised by a different frequency content, are applied at the bedrock of the FE model. The principal findings of the sensitivity analysis are:

- Simply scaling the ground motion records at the same peak acceleration can induce very different levels of shear strain in the deposit, thus affecting the propagation of the accelerations in the soil and, consequently, the forces in the tunnel lining. This is due to the importance of the spectral shape of the input motion in non-linear soil response, as PGA is not a good indicator of the strength and frequency content of the seismic motion.
- The implementation of elasto-plastic models allows to predict permanent increments of hoop force, bending moment and shear force at the end of the motions due to the accumulation of plastic deformation in the soil deposit during the earthquakes.
- The soil structure degradation rate does not particularly affect the wave propagation in the deposit, but leads to higher shear strain levels in the soil deposit due to its softer behaviour.
- A rise in the maximum and minimum values of the lining forces attained during the earthquake motions is predicted when higher rates of soil structure degradation are accounted for.

- When a higher degree of destructuration is allowed to occur in the dynamic simulations, a consistent increase in the hoop force and bending moment increments accumulated in the tunnel lining can be observed.

Although a natural clay deposit is characterised by high stiffness and peak strength due to its initial degree of structure, the earthquake loading can induce sufficient stiffness degradation in the soil associated to strain-softening processes, which, in turn, facilitate the transmission of higher loads to the tunnel lining. Therefore, the paper highlights for the first time the importance of considering structure degradation in the assessment of the dynamic response of shallow tunnels constructed in structured clayey deposits as it can significantly control the magnitude of the tunnel lining forces and, in consequence, the overall tunnel design.

Acknowledgments

The Authors would like to thank Daniela Menozzi from the University of Rome "La Sapienza" and Fabio Maria Soccodato from the University of Cagliari for providing some of the Avezzano Clay data presented in the PhD thesis of Marco D'Elia. The Authors would also like to acknowledge the anonymous reviewers for their valuable comments and suggestions.

References

[1] United Nations, Department of Economic and Social Affairs, Population Division (2015) World Urbanization Prospects: The 2014 Revision, (ST/ESA/SER.A/366).

[2] Hashash YMA, Hook JJ, Schmidt B, Yao JJ (2001) Seismic design and analysis of underground structures. Tunnelling and Underground Space Technology, 16:247-93.

[3] Yashiro K, Kojima Y, Shimizu M (2007) Historical earthquake damage to tunnels in Japan and case studies of railway tunnels in the 2004 Niigataken-Chuetsu earthquake. Quarterly Report of Railway Technical Research Institute, 48(3):136-41.

[4] Wang WL, Wang TT, Su JJ, Lin CH, Seng CR, Huang TH (2001) Assessment of damage in mountain tunnels due to the Taiwan Chi-Chi earthquake. Tunnelling and Underground Space Technology, 16:133-150.

[5] Li T (2012) Damage to mountain tunnels related to the Wenchuan earthquake and some suggestions for aseismic tunnel construction. Bulletin of Engineering Geology and the Environment, 71:297-308.

[6] Owen GN, Scholl RE (1981) Earthquake engineering of large underground structures. In: Report No. FHWA/RD-80/195. Federal Highway Administration and National Science Foundation.

[7] Penzien J (2000) Seismically induced racking of tunnel linings. Earthquake Engineering and Structural Dynamics, 29:683-91.

[8] Hwang RN, Lysmer J (1981) Response of buried structures to traveling waves. Journal of the Geotechnical Engineering Division, 107(GT2):183-200.

[9] Wang JN (1993) Seismic design of tunnels: a state-of-the-art approach. Monograph 7. New York, Parsons, Brinckerhoff: Quade & Diuglas Inc.

[10] Penzien J, Wu CL (1998) Stresses in linings of bored tunnels. Earthquake Engineering and Structural Dynamics, 27:283-300.

[11] Khoshnoudian F, Shahrour I (2002) Numerical analysis of the seismic behaviour of tunnels constructed in liquefiable soils. Soils and Foundations, 42(6):1-8.

[12] Pakbaz MC, Yareevand A (2005) 2-D analysis of circular tunnel against earthquake loading. Tunnelling and Underground Space Technology, 20:411-417.

[13] Liu H, Song E (2005) Seismic response of large underground structures in liquefiable soils subjected to horizontal and vertical earthquake excitations. Computers and Geotechnics, 32:223-244.

[14] Amorosi A, Boldini D (2009) Numerical modelling of the transverse dynamic behaviour of circular tunnels in clayey soils. Soil Dynamics and Earthquake Engineering, 29(6):1059-1072.

[15] Azadi M, Mir Mohammad Hosseini SM (2010) Analyses of the effect of seismic behavior of shallow tunnels in liquefiable grounds. Tunnelling and Underground Space Technology, 25:543-552.

[16] Shahrour I, Khoshnoudian F, Sadek M, Mroueh H (2010) Elastoplastic analysis of the seismic response of tunnels in soft soils. Tunnelling and Underground Space Technology, 25:478-482.

[17] Kontoe S, Zdravkovic L, Potts DM, Menkiti CO (2011) On the relative merits of simple and advanced constitutive models in dynamic analysis of tunnels. Géotechnique, 61:815-829.

[18] Stamos AA, Beskos DE (1995) Dynamic analysis of large 3-D underground structures by the BEM. Earthquake Engineering and Structural Dynamics, 24(6): 917-34.

[19] Stamos AA, Beskos DE (1996) 3-D seismic response of long lined tunnels in half- space. Soil Dynamics and Earthquake Engineering, 15:111-8.

[20] Yang D, Naesgaard E, Byrne PM, Adalier K, Abdoun T (2004) Numerical model verification and calibration of George Massey Tunnel using centrifuge models. Canadian Geotechnical Journal, 41:921-42.

[21] Gazetas G, Gerolymos N, Anastasopoulos I (2005) Response of three Athens metro underground structures in the 1999 Parnitha earthquake. Soil Dynamics and Earthquake Engineering, 25:617-33.

[22] Hatzigeorgiou GD, Beskos DE (2010) Soil-structure interaction effects on seismic inelastic analysis of 3-D tunnels. Soil Dynamics and Earthquake Engineering, 30:851-861.

[23] Rouainia M, Muir Wood D (2000) A kinematic hardening constitutive model for natural clays with loss of structure. Géotechnique, 50:153-164.

[24] Gonzáles NA, Rouainia M, Arroyo M, Gens A (2012) Analysis of tunnel excavation in London Clay incorporating soil structure. Géotechnique, 62(12):1095-1109.

[25] Panayides S, Rouainia M, Muir Wood D (2012) Influence of degradation of structure on the behaviour of a full-scale embankment. Canadian Geotechnical Journal, 49:344-356.

[26] Elia G, Rouainia M (2013) Seismic performance of earth embankment using simple and advanced numerical approaches. Journal of Geotechnical and Geoenvironmental Engineering, 139(7):1115-1129.

[27] Elia G, Rouainia M (2014) Performance evaluation of a shallow foundation built on structured clays under seismic loading. Bulletin of Earthquake Engineering, 12(4):1537-1561.

[28] PLAXIS 2D (2015) Reference Manual. Plaxis bv, Delft, The Netherlands.

[29] Zhao J, Sheng D, Rouainia M, Sloan SW (2005) Explicit stress integration of complex soil models. International Journal for Numerical and Analytical Methods in Geomechanics, 29(12):1209-1229.

[30] Burghignoli A, D'Elia M, Miliziano S, Soccodato FM (1999) Analisi dei cedimenti di un silo fondato su terreni argillosi cementati. Rivista Italiana di Geotecnica, 3:23-36.

[31] D'Elia M. (2001) Comportamento meccanico in condizioni cicliche e dinamiche di un'argilla naturale cementata. PhD Thesis, University of Rome "La Sapienza", Rome, Italy.

[32] Burghignoli A, Miliziano S, Soccodato FM (2010) Cementation effects in two lacustrine clayey soils. Geotechnical and Geological Engineering, 28:815-833.

[33] D'Elia M, Miliziano S, Soccodato FM, Tamagnini C (1999) Observed and predicted behaviour of a silo founded on a cemented soft clayey soil. In: Jamiolkowski, Lancellotta, Lo Presti Eds., Pre-failure deformation characteristics of geomaterials, Balkema, Rotterdam, pp. 741-748.

[34] Burghignoli A, Cocciuti M, Miliziano S, Soccodato FM (2003) Evaluation of the advanced constitutive modelling for cemented clay soils: a case history. Mathematical and Computer Modelling, 37:631-640.

[35] Viggiani GMB, Atkinson JH (1995) Stiffness of fine-grained soil at very small strains. Géotechnique, 45(2):249-265.

[36] Elia G, Rouainia M (2016) Investigating the cyclic behaviour of clays using a kinematic hardening soil model. Soil Dynamics and Earthquake Engineering, 88:399-411.

[37] Zienkiewicz OC, Chan AHC, Pastor M, Schrefler BA, Shiomi T (1999) Computational geomechanics (with special reference to earthquake engineering). Wiley, Chichester.

[38] Amorosi A, Boldini D, Elia G (2010) Parametric study on seismic ground response by finite element modelling. Computers and Geotechnics, 37(4):515-528.

[39] Kuhlemeyer RL, Lysmer J (1973) Finite element method accuracy for wave propagation problems. Journal of the Soil Mechanics and Foundations Division, 99(5):421-427.

[40] Mair RJ (1996) Settlement effects of bored tunnels. In: Proc. Int. Symposium on Geotechnical Aspects of Underground Construction in Soft Ground. London, Balkema, pp. 43-53.

[41] Roesset JM (1977) Soil amplification of earthquakes. In Desai and Christian Eds., Numerical Methods in Geotechnical Engineering, McGraw-Hill, New York, pp. 639-682.

[42] Arias A (1970) A measure of earthquake intensity. In Hansen Ed., Seismic design for nuclear power plants, Massachusetts Institute of Technology Press, Cambridge, Mass., pp. 438-483.

[43] Trifunac MD, Brady AG (1975) A study of the duration of strong earthquake ground motion. Bulletin of the Seismological Society of America, 65:581-626.

Parameter/ symbol	Physical contribution/meaning	Avezzano Clay
M	Critical state stress ratio for triaxial compression	1.42
λ^*	Slope of normal compression line in ln$v$-ln$p$ compression plane	0.11
κ^*	Slope of swelling line in ln$v$-ln$p$ compression plane	0.016
R	Ratio of size of bubble and reference surface	0.4
B	Stiffness interpolation parameter	15.0
ψ	Stiffness interpolation exponent	1.45
η_0	Anisotropy of initial structure	**0.0**
r_0	Initial degree of structure	5.2
A^*	Parameter controlling relative proportion of distorsional and volumetric destructuration	0.2
k	Parameter controlling rate of destructuration with damage strain	1.5 / 5.0

Table 1. *RMW* parameters

Station	Earthquake	Component	Magnitude (M_w)	Arias intensity I_a (m/s)	Epicentral distance (km)	Duration T_{90} (s)	a_{max} (g)	v_{max} (m/s)
Assisi-Stallone	Umbria-Marche (1997)	EW	6.0	0.2793	21.6	5.98	0.188	0.102
Ulcinj-Hotel Albatros	Montenegro (1979)	NS	6.9	0.7289	19.7	12.22	0.181	0.176

Table 2. Main characteristics of the selected earthquake signals

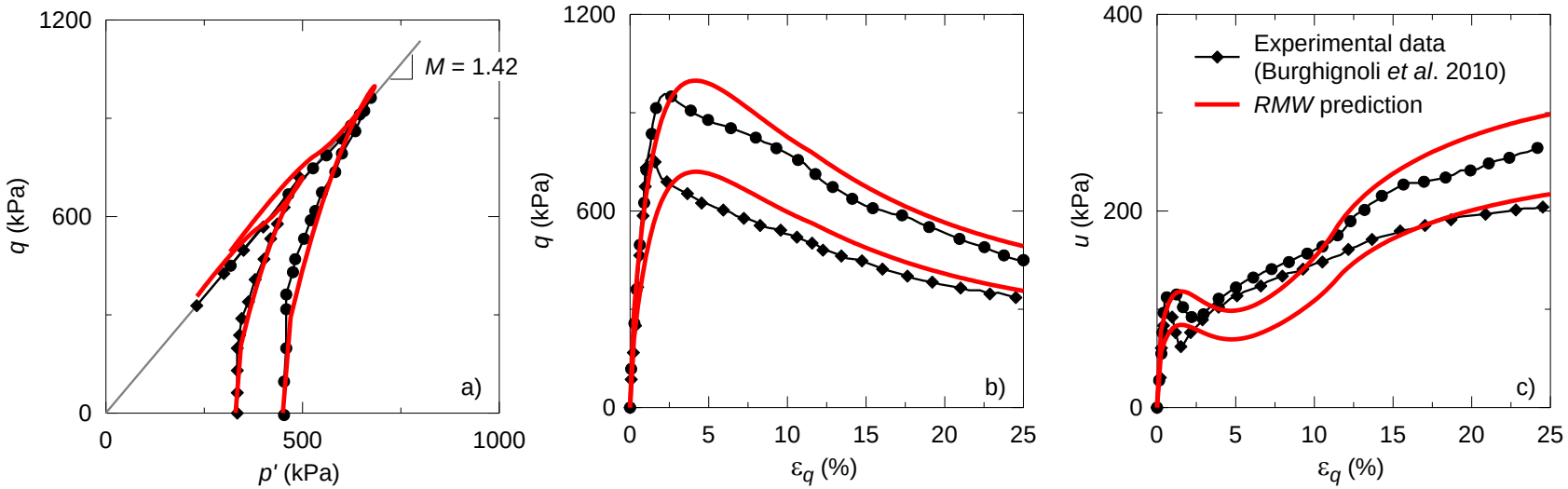

Figure 1. Comparison between *RMW* predictions and laboratory data on Avezzano Clay: (a) stress path; (b) stress-strain response; (c) pore pressure-strain response.

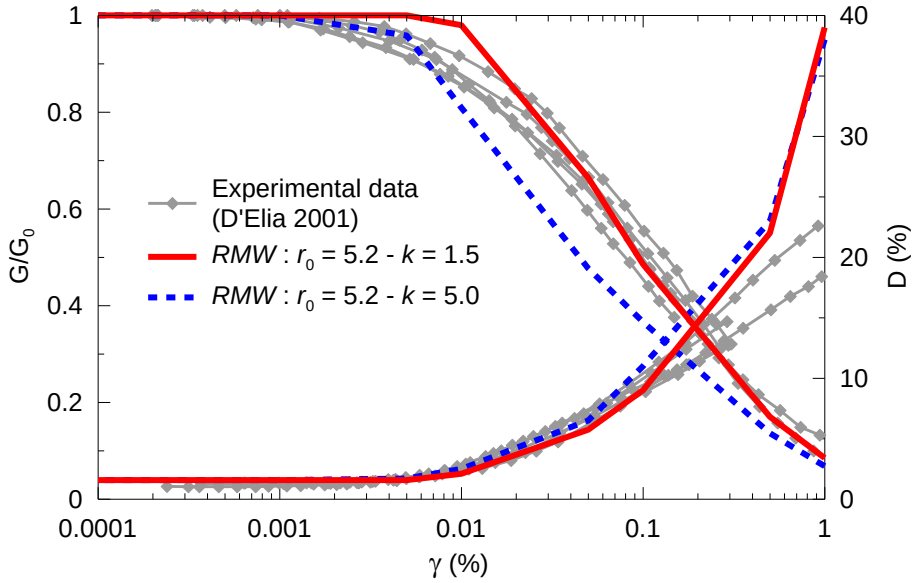

Figure 2. Comparison between *RMW* predictions obtained for two different destructuration rates (i.e. *k* values) and normalised modulus decay and damping curves for Avezzano Clay.

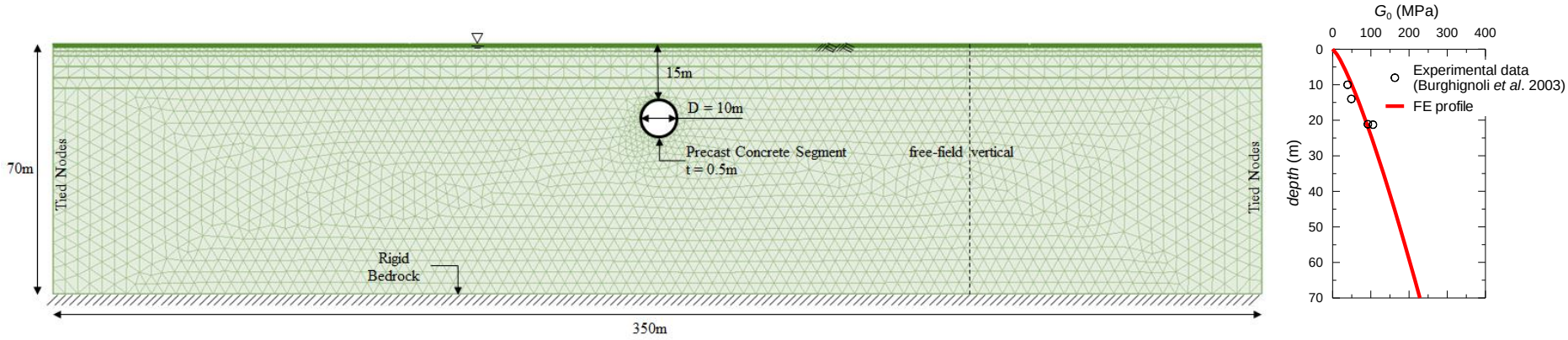

Figure 3. Adopted FE model and boundary conditions for the dynamic simulations.

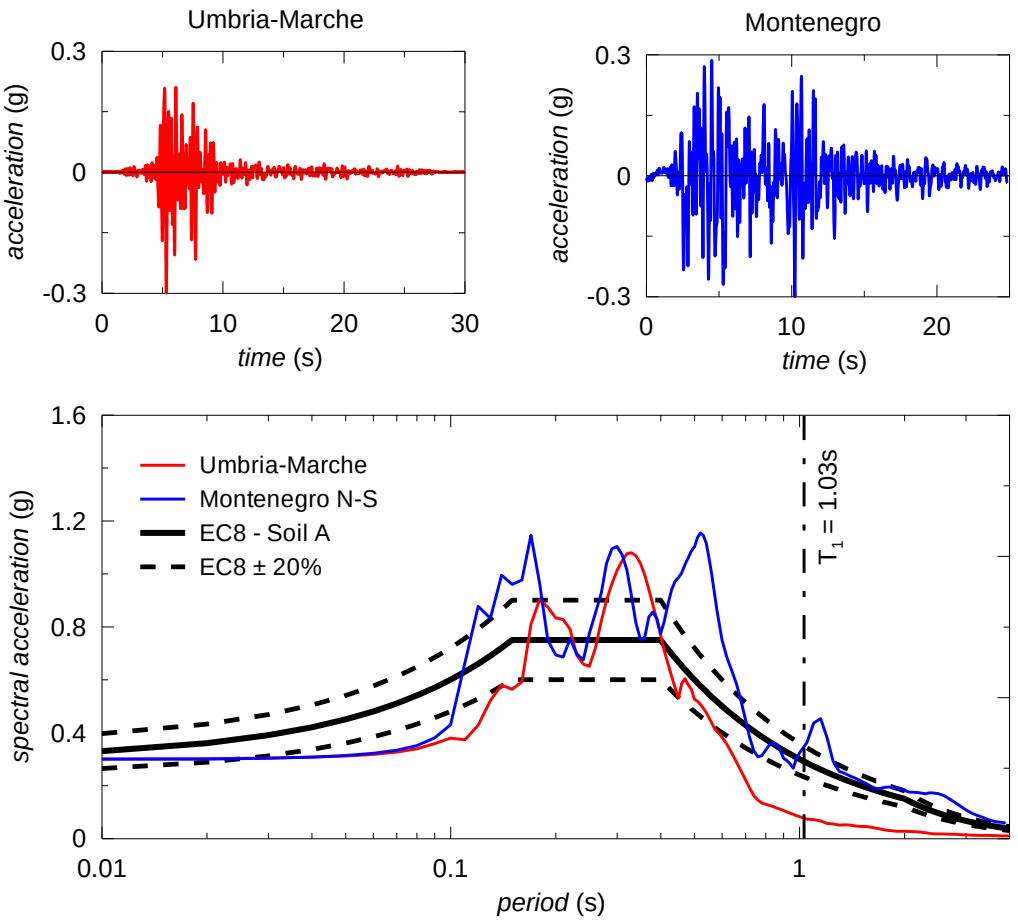

Figure 4. Input motion acceleration time histories and response spectra.

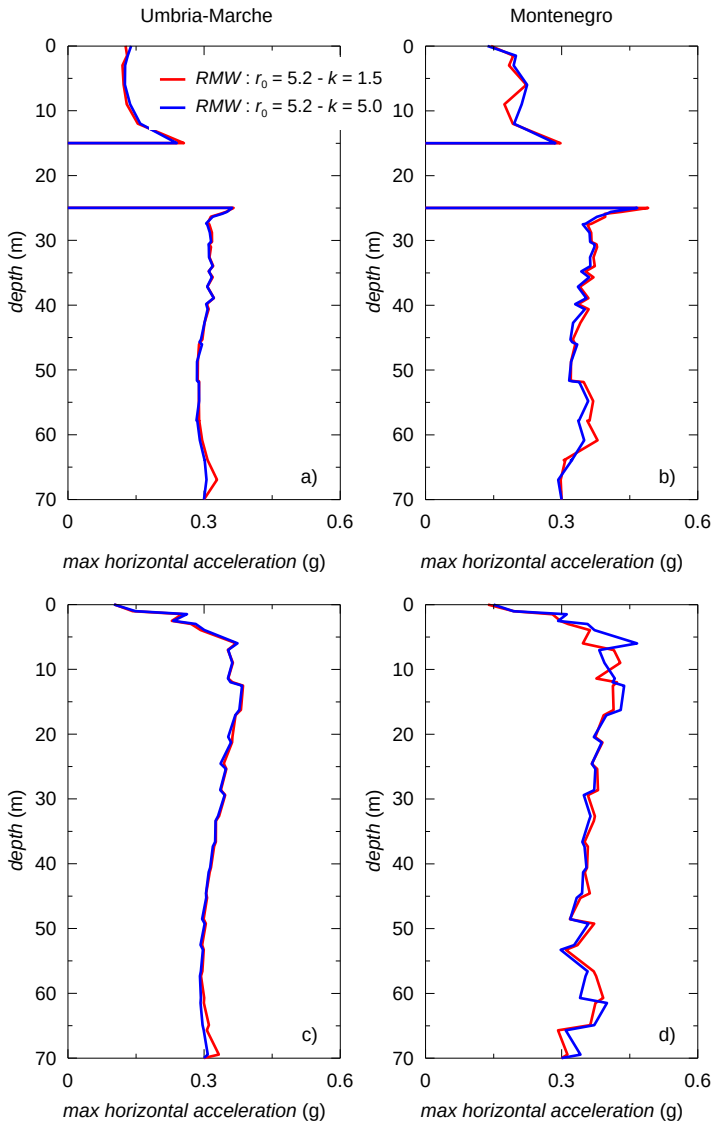

Figure 5. Influence of structure degradation rate on the profiles of max accelerations recorded along the tunnel vertical and in free field conditions during the: (a-c) Umbria-Marche; (b-d) Montenegro event.

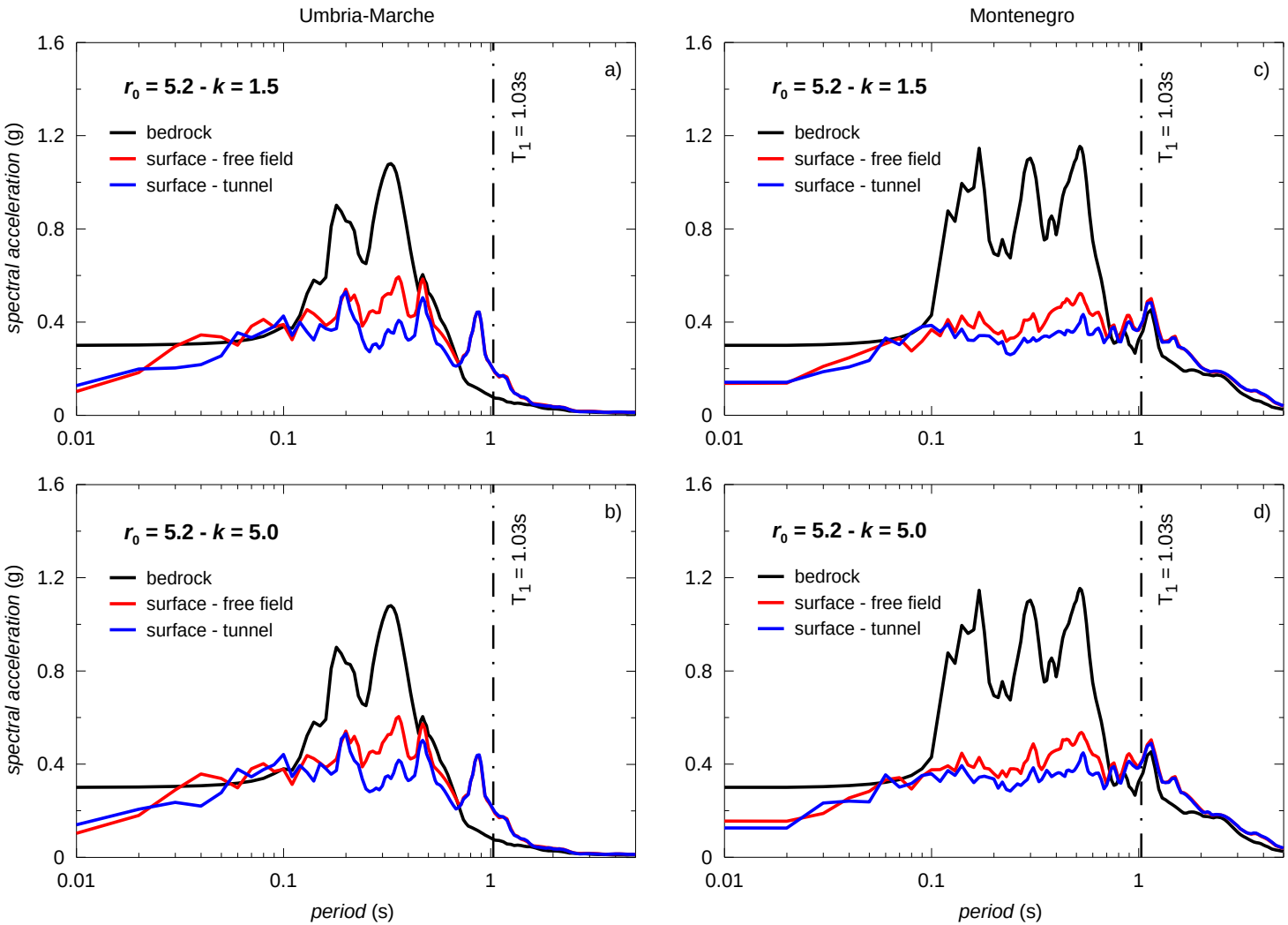

Figure 6. Comparison of response spectra recorded at bedrock and at surface during the: (a) Umbria-Marche; (b) Montenegro event for different destructuration rates.

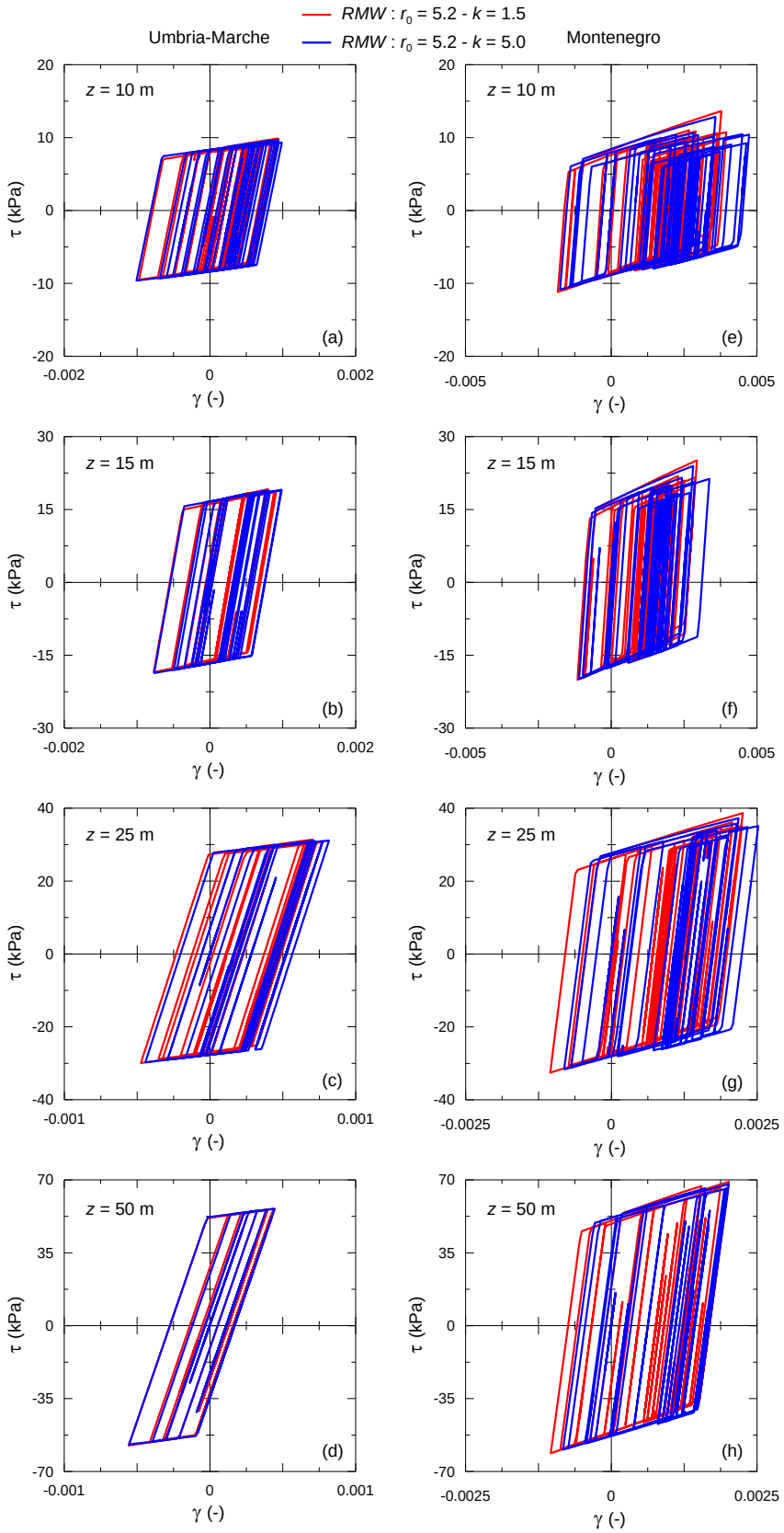

Figure 7. Stress-strain curves during the: (a-d) Umbria-Marche; (e-h) Montenegro event for different destructuration rates.

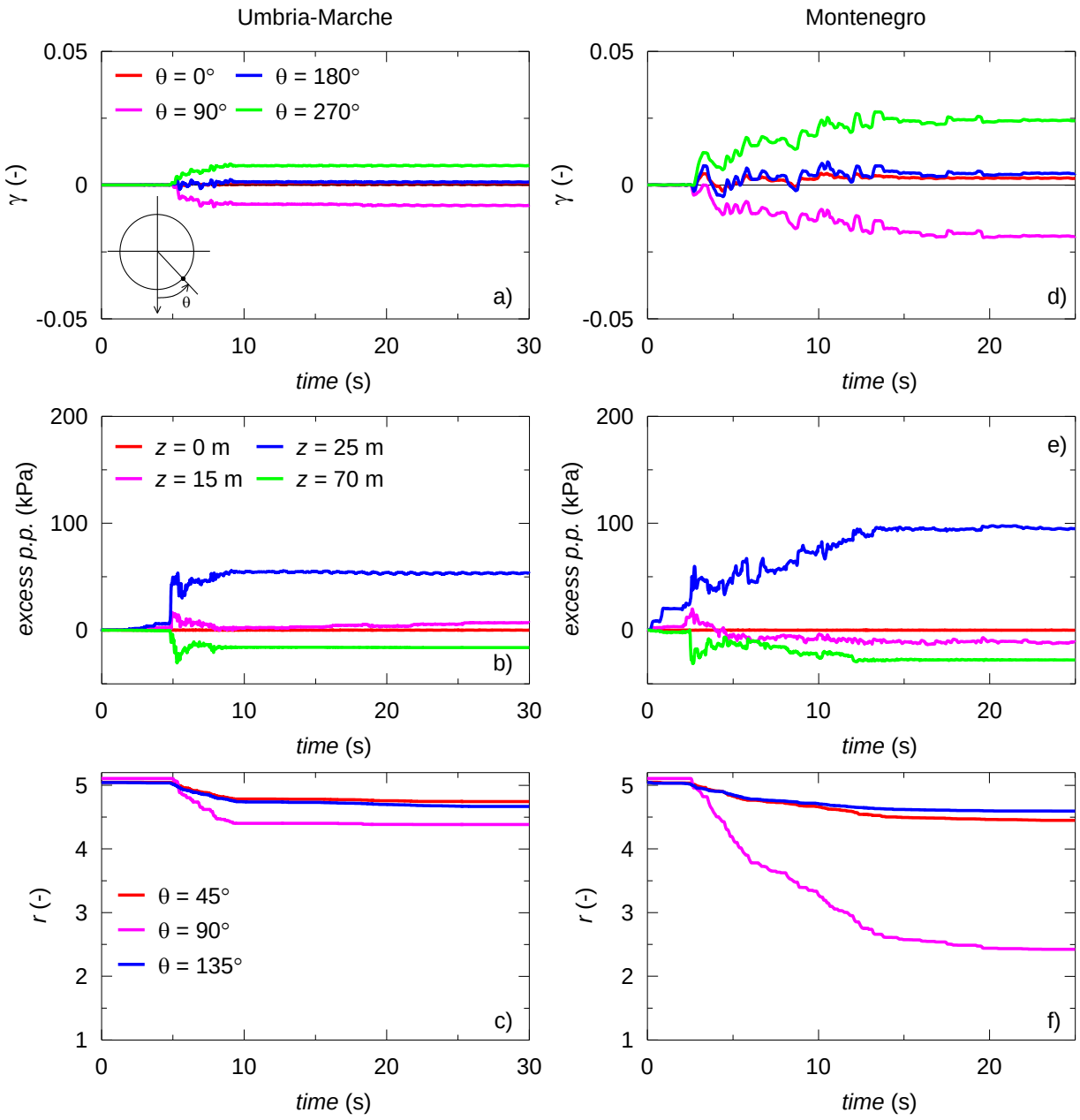

Figure 8. Time histories of shear strain, excess pore pressure and *RMW* soil structure parameter *r* during the: (a-c) Umbria-Marche; (d-f) Montenegro event for a destructuration rate k = 1.5.

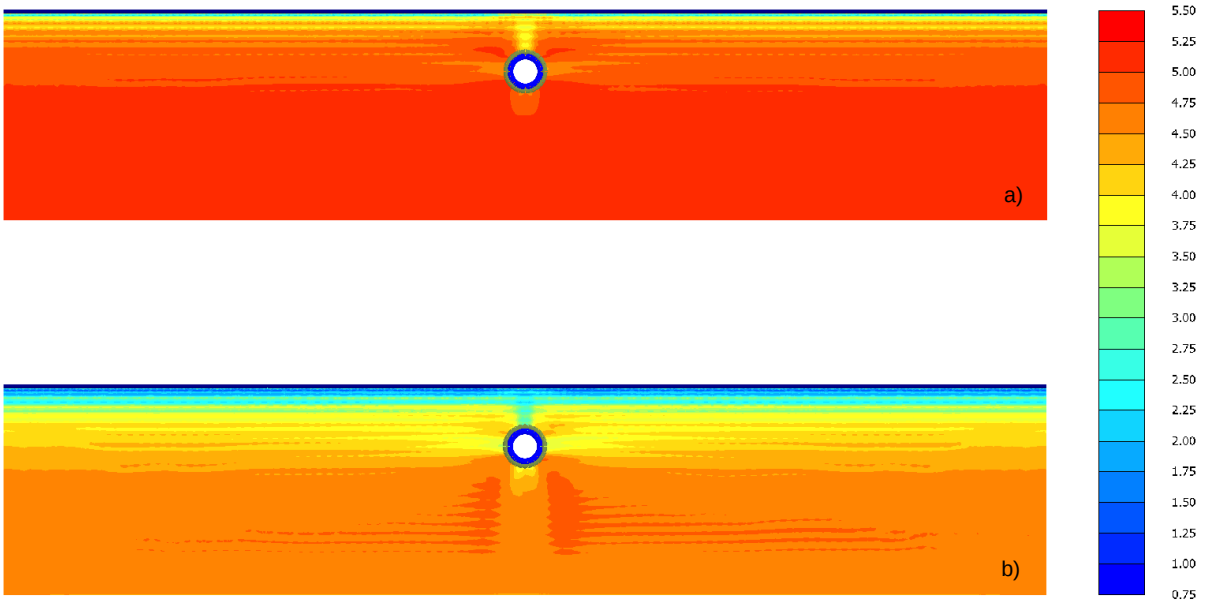

Figure 9. Contours of the *RMW* parameter r at the end of the: (a) Umbria-Marche; (b) Montenegro event for a destructuration rate k = 1.5 (note that r_0 is equal to 5.2 in both cases).

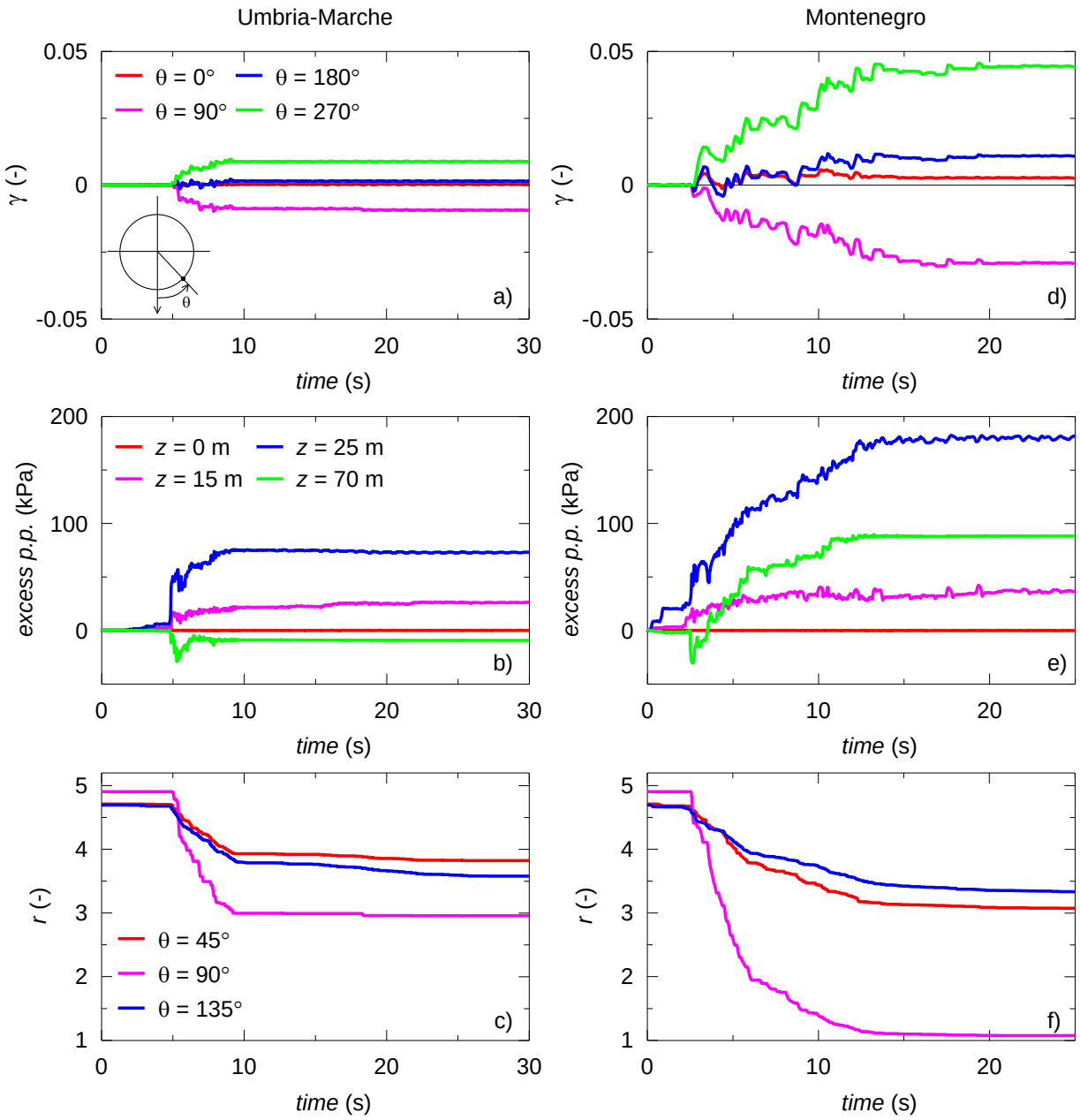

Figure 10. Time histories of shear strain, excess pore pressure and *RMW* soil structure parameter *r* during the: (a-c) Umbria-Marche; (d-f) Montenegro event for a destructuration rate k = 5.0.

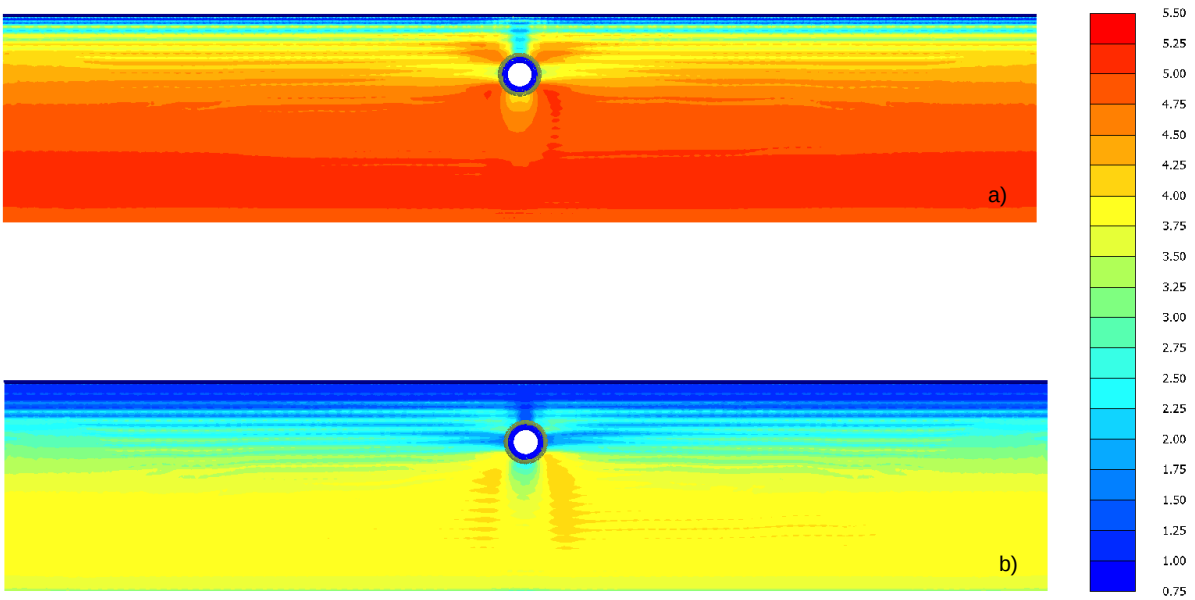

Figure 11. Contours of the *RMW* parameter r at the end of the: (a) Umbria-Marche; (b) Montenegro event for a destructuration rate k = 5.0 (note that r_0 is equal to 5.2 in both cases).

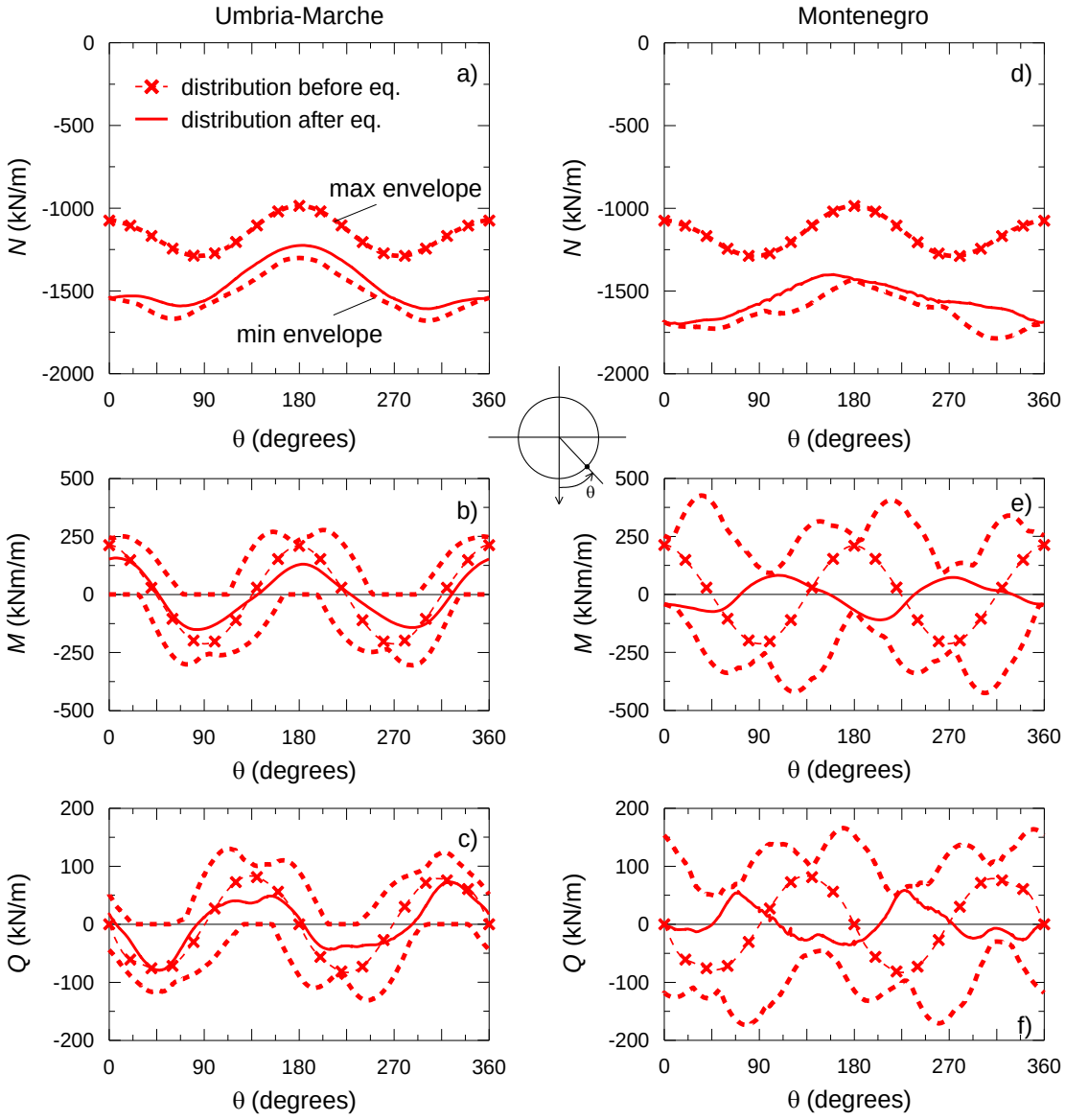

Figure 12. Distribution of hoop force (*N*), bending moment (*M*) and shear force (*Q*) before and after the: (a-c) Umbria-Marche; (d-f) Montenegro event for a destructuration rate $k = 1.5$.

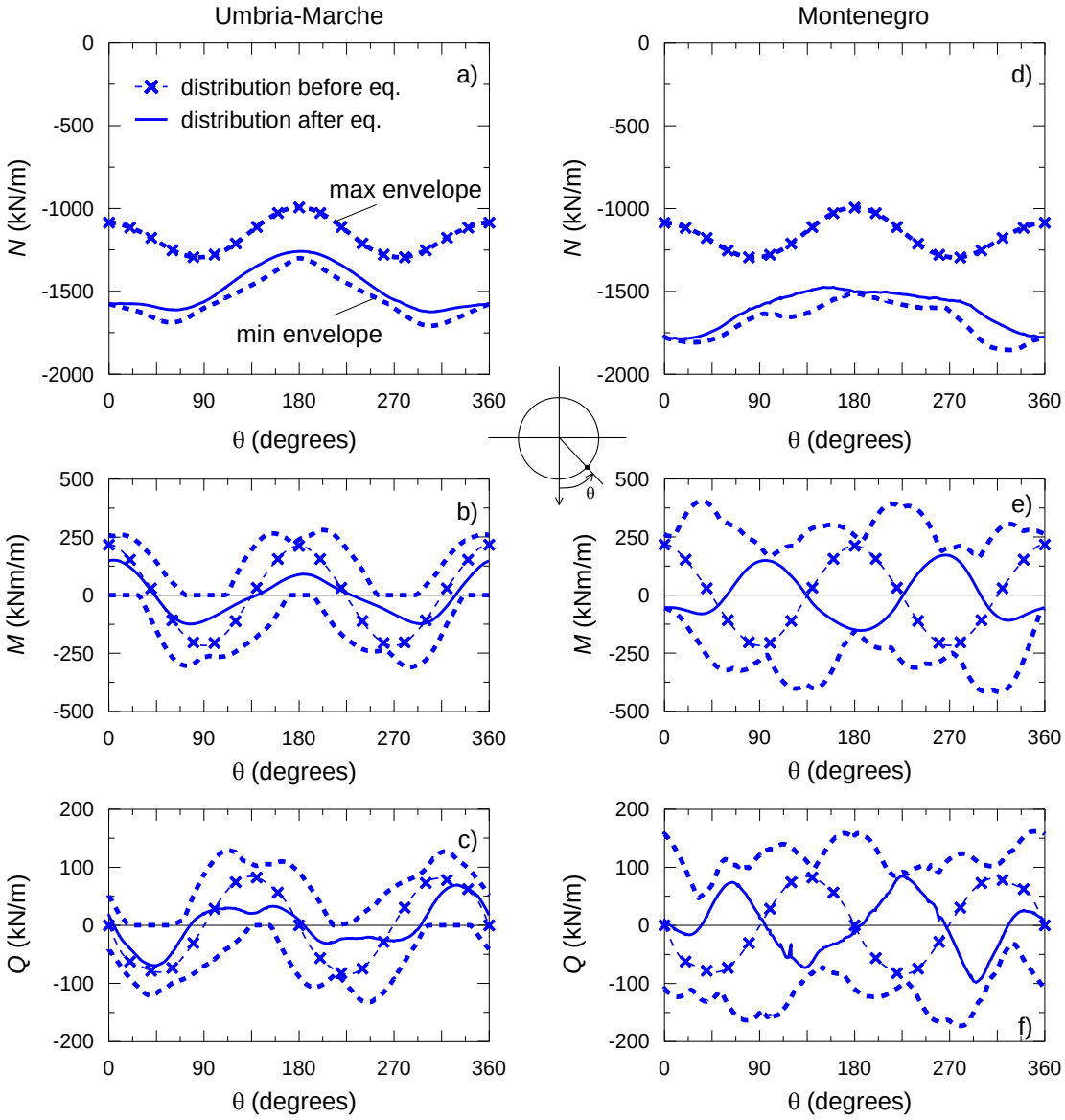

Figure 13. Distribution of hoop force (*N*), bending moment (*M*) and shear force (*Q*) before and after the: (a-c) Umbria-Marche; (d-f) Montenegro event for a destructuration rate $k = 5.0$.

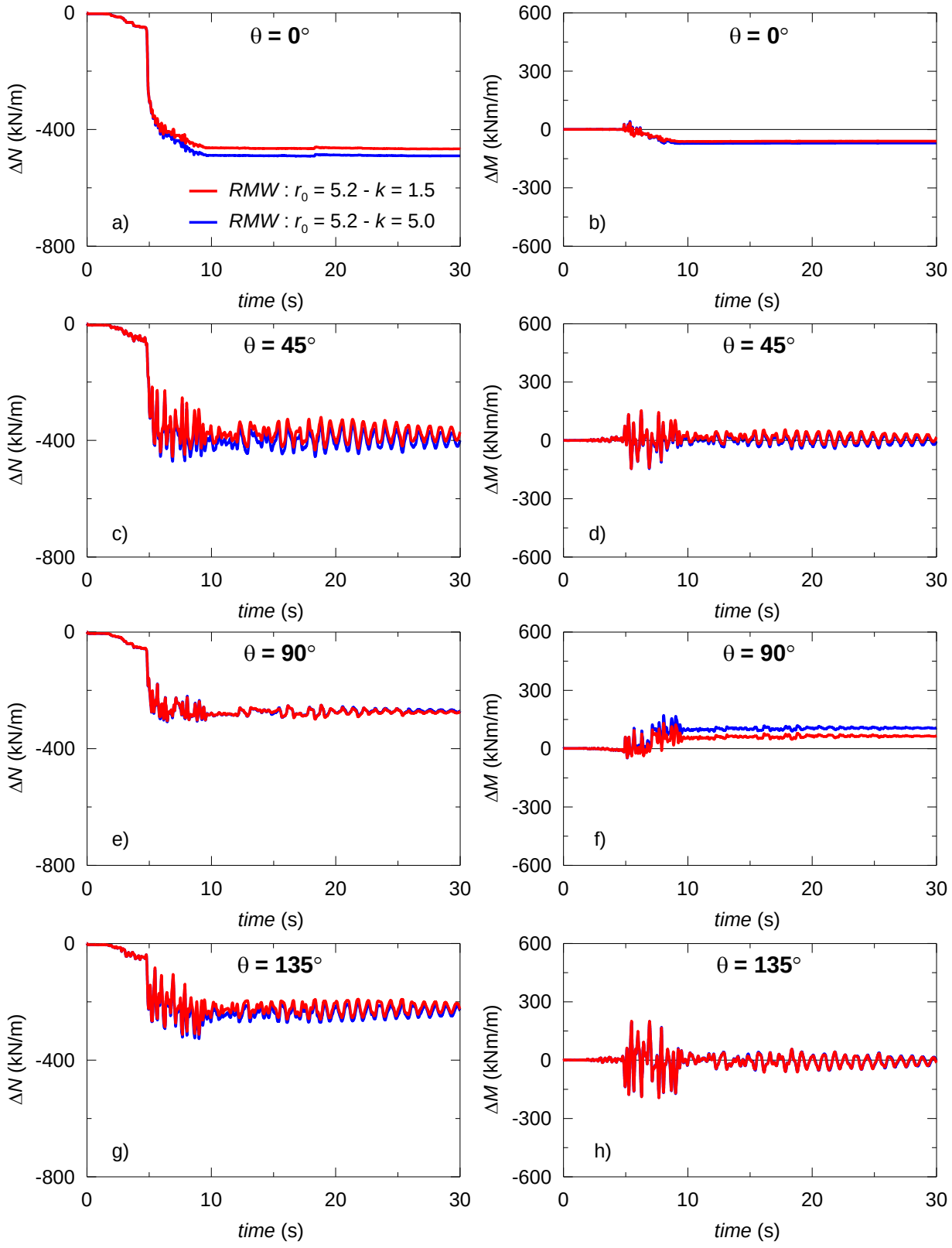

Figure 14. Influence of structure degradation rate on the time histories of hoop force and bending moment increments during the Umbria-Marche event for: (a-b) θ = 0°; (c-d) θ = 45°; (e-f) θ = 90°; (g-h) θ = 135°.

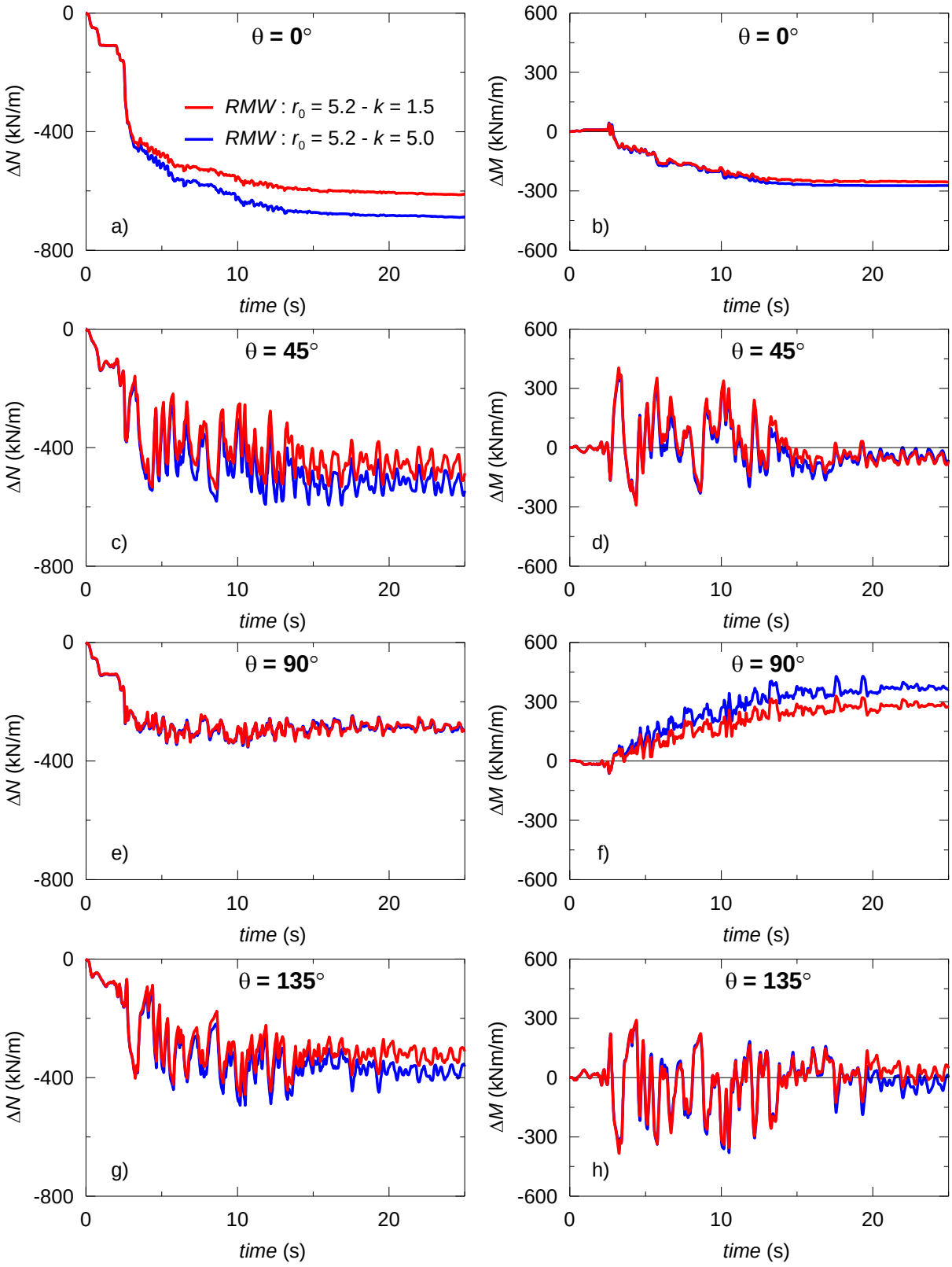

Figure 15. Influence of structure degradation rate on the time histories of hoop force and bending moment increments during the Montenegro event for: (a-b) θ = 0°; (c-d) θ = 45°; (e-f) θ = 90°; (g-h) θ = 135°.